Chinese Herbal Medicines 16 (2024) 466–480

Contents lists available at ScienceDirect

Chinese Herbal Medicines

journal homepage: www.elsevier.com/locate/chmed

Original Article

Identification and characterization of chemical constituents in Mahuang Guizhi Decoction and their metabolites in rat plasma and brain by UPLC-Q-TOF/MS

Ping Wei [a,1], Shiying Huang [b,1], Juan Yang [a], Mo Zhao [a], Qiugu Chen [b], Xiaoyu Deng [a], Jianping Chen [b,*], Yisheng Li [c,*]

[a] Pingshan District Maternal & Child Healthcare Hospital of Shenzhen, Pingshan General Hospital of Southern Medical University, Shenzhen 518118, China
[b] Shenzhen Key Laboratory of Hospital Chinese Medicine Preparation, Shenzhen Traditional Chinese Medicine Hospital, The Fourth Clinical Medical College of Guangzhou University of Chinese Medicine, Shenzhen 518000, China
[c] Shenzhen Longgang Otorhinolaryngology Hospital, Shenzhen 518100, China

ARTICLE INFO

Article history:
Received 18 May 2023
Revised 15 December 2023
Accepted 22 January 2024
Available online 21 May 2024

Keywords:
chemical constituents
Mahuag Guizhi Decoction
metabolites
rat plasma and brain
UPLC-Q-TOF-MS

ABSTRACT

Objective: Mahuang Guizhi Decoction (MGD), an essential herbal pair in traditional Chinese medicine, is able to release cold, fever and asthma, mainly containing alkaloids, flavonoids, phenylpropanoids and amino acids. However, the absorption and distribution of these four category compounds *in vivo* still remained unclearly.

Methods: In our research, we utilized UPLC-Q-TOF-MS technique to identify the constituents within MGD, as well as the prototypes of MGD and their metabolites absorbed in plasma and brain. We further profiled the drug-time curve of prototypes and metabolites of MGD both in plasma and brain.

Results: Our results showed that 105 constituents were characterized in MGD. Thirty of them could be absorbed into blood, and ten of them could be distributed into brain. We also discovered eight new bio-transformed metabolites in blood, and a half of which could pass through the blood–brain barrier. In addition, all components detected *in vivo* could be absorbed and distributed immediately.

Conclusion: These findings provide an approachable method to analyze the potential bio-active compounds in MGD and their *in vivo* behaviors, which could promote the efficacious material basis study of MGD and the security of clinical utilization.

1. Introduction

Traditional Chinese medicine (TCM) formulas, being composed by one or more drugs of plant or animal origin, have been used as major remedies in China and other Asian countries for thousands of years with reliable efficacies. Mahuang Guizhi Decoction (MGD), a therapeutic herbal pair formula consisting of *Ephedrae Herba* (Mahuang in Chinese, EH) and *Cinnamomi Ramulus* (Guizhi in Chinese, CR) with the ratio of 3 to 2, has been clinically used in releasing exterior cold to ameliorate asthma, influenza virus, inflammation and pyrexia (Fu et al., 2018; Wei et al., 2014). Considering the complicated composition in Chinese herbal formula, multi-components are regarded as the typical characteristic of TCM. Alkaloid, flavonoid, phenylpropanoid and organic acid are considered as the potential bio-active ingredients of MGD, and some of them including prototypes or their metabolites have been proved to be absorbed into blood and play roles through various pathways (Fan et al., 2020; Mu et al., 2019). However, ephedra alkaloids have been reported to take its effect on nervous centralis, which would occur side effect, such as addition of neural disease-related functions and damage to the balance of neurotransmitters (Kim, Cao, & Kim, 2011; Niu, Zheng, & Xu, 2020). In TCM prescriptions, certain herbs are composed together in order to enhance the efficacies or reduce the potential toxicity (Zheng et al., 2023a, 2023b). Previous studies had proved that CR coupled with EH could decrease the oxidative damage in the prefrontal cortex compared to EH used only (Niu, Zheng, & Xu, 2020; Zheng et al., 2015). In addition, combination of these two herbs resulted in the change of pharmacokinetic parameters for three phenylpropanoids compared to use CR only (Wei et al., 2017). As a result, understanding the chemical absorption and brain distribution of MGD as well as its metabolites are essential for the MGD *in vivo* mechanism research.

* Corresponding authors.
E-mail addresses: lycjp@126.com (J. Chen), lys607@sohu.com (Y. Li).
[1] These authors contributed equally to this work.

https://doi.org/10.1016/j.chmed.2024.01.006
1674-6384/

Pharmacokinetics is a typical method to explore *in vivo* dynamic change of drugs, including their absorption, distribution, metabolism and excretion. Owing to the multi-components with vary contents in a TCM formula, a sensitive and accurate technology is crucial for chemical analysis, like ultra-high performance liquid chromatography with quadrupole time-of-flight mass spectrometry (UPLC-Q-TOF-MS) and gas chromatography-triple quadrupole mass spectrometry (GC–MS/MS) (Chen et al., 2021; Xiang et al., 2016). Recently, coupled by those advanced analytical approaches, a growing number of research has been conducted to analyze the blood concentration and organ distribution of the constituents and their metabolites, which presented the evidence of the discovery of the effective substance within TCM formula (Lin et al., 2022; Liu et al., 2021; Xu, Liu, Wu, & Zhou, 2020). In addition, some previous studies have reported the chemical profiles and their certain metabolism of EH and CR in other formula (Wan et al., 2020; Yuan et al., 2017). Moreover, we had explored the pharmacokinetics including biological half-life ($t_{1/2}$), the area under the curve (*AUC*), the peak drug concerntration (C_{max}) and the time to peak (T_{max}) of five different ephedrine alkaloids *in vivo* after oral treatment MGD (Wei et al., 2014). However, systematic research focusing on the combination of MGD especially its *in vivo* metabolites has been rarely investigated.

Hence, in our current studies, an UPLC-QTOF/MS approach was established to profile the chemical constituents of MGD and elaborate on the absorbed constituents and their metabolites in rat plasma and brain after oral administration of MGD. Moreover, the drug-time curves of prototypes and their metabolites in rat plasma and brain were also depicted. It is expected that these findings could provide helpful information for the follow-up exploration of the effective substance mechanism as well as establishment of quality control method based on *in vivo* study of MGD, whih could support for clinical application of MGD.

2. Materials and methods

2.1. Chemicals and regents

Gallic acid (110831–201204), protocatechuic acid (110809–201906), *trans*-cinnamic acid (110786–201604), catechin (110877–201604), epicatechin (110878–201703), ephedrine (171241–201809), pseudoephedrine (171237–201510), (−)-*N*-methylephedrine (171247–201502) were purchased from National Institutes for Food and Drug Control (Beijing, China), coumarin (wkq21030207) and syringaldehyde (200910) from Sichuan Victory Biology Co., Ltd. (Chengdu, China) and Guangzhou Qiyun Biology Co., Ltd. (Guangzhou, China). Acetonitrile, methanol, water and formic acid (LC-MS grade) were purchased from Fisher Scientific (Fair Lawn, New Jersey, USA).

2.2. Preparation of MGD

Ephedrae Herba (the herbaceous stems of *Ephedra sinica* Stapf; lot No. 201000051) and *Cinnamomi Ramulus* (the twig of *Cinnamomum cassia* Presl; lot No. 202011068) were offered by Kangmei Pharmaceutical Co., Ltd. (Puning, China) and Zhongshan Zhengdexiang Pharmaceutical Co., Ltd. (Zhongshan, China). The materials were authenticated by Dr. Jianping Chen according to the *Pharmacopoeia of the People's Republic of China* (2020 Edition).

MGD was prepared as previously described (Wei et al., 2014). Briefly, 90 g EH was emerged into 2.4 L water for 30 min at room temperature, followed by boiling. After 20 min extraction, 60 g CR was added for another 30 min boiling. At last, the MGD extraction was filtered, concentrated and dried into powder.

2.3. Animals

Male Wistar rats (200 ± 10 g, permitted No. 20221124Aazz0100000791) obtained from Qinglongshan Mutipliying Farm (Jiangsu, Nanjing, China) were used to explore the MGD and its metabolites absorption and distribution *in vivo*. After 7 days' adaption in room temperature (22 ± 1) °C with 12 h light circle, all animals were intervened orally with 6.0 g/kg MGD powder dissolved in water after 12 h fasting.

At 0, 15, 30, 60, 90, 120, 240 and 360 min, blood sample was collected by orbital venous plexus into EP tubes which were added 10 μL heparin sodium in advanced. The collected blood samples were centrifuged at 4 500 r/min for 5 min and supernatant was transferred, namely plasma. The whole brain issue was collected at 0, 30, 60, 90 and 120 min, using 20% ethyl carbamate to narcotize.

2.4. Sample pretreatment

2.4.1. MGD samples

MGD powder was weighted 0.1 g accurately and extracted twice by ultrasound with 10 mL 70% methanol, 30 min for each time. After collecting the ultrasonic filtrate, supernatant (2 mL) was dried by N_2 and redissolved by the same volume water. Next, the mixture was added onto the well-prepared C_{18} solid phase extraction column (3 cc, 500 mg, Waters, Ireland, WAT020805) and eluded by 1 mL water, followed by 2 mL methanol and collecting the methanol eluent. Before the analysis, the eluent was centrifugated at 12 000 r/min for 10 min, and 400 μL of supernatant was dried by N_2 and redissolved by 70% methanol.

2.4.2. Plasma and brain samples

Plasma from three different rat samples was put together at each time point and 400 μL ice acetonitrile was added into 200 μL well-mixed plasma followed by a completed vortex. As for brain sample, 100 mg was grinded with 800 μL methanol in high-speed grinding miller (Jingxin, Shanghaijingxin, Shanghai, China). The well-prepared plasma or brain mixture would experience a 15 min centrifugation at 4 ℃ with 130 000 r/min. The supernatant (400 μL) of it was transferred and dried by N_2. Finally, all remnant was redissolved by 50% acetonitrile and centrifugated again before analysis.

2.5. UPLC-Q-TOF-MS analysis

The chromatographic peaks were separated on SCIEX Exion LC (AB Sciex, Foster City, CA, USA) by Waters Acquity HSS T3 column (150 mm × 2.1 mm, 1.8 μm), using 0.1% formic acid (A)-acetonitrile (B) at a flowing rate of 0.3 mL/min by a gradient elution: 0–5 min, 3%–8% B; 5–11 min, 8%–30% B; 11–20 min, 30%–80% B; 20–21 min, 80%–95% B. The column temperature was 35 °C, and 2 μL of each sample would be injected into the analytical system.

The corresponding mass information was performed on X500B Q-TOF mass spectrometer (AB Sciex, Foster City, CA, USA) equipped with ESI source. Mass spectra were acquired in both positive and negative ion modes with mass scan range 100–1 250 *m*/*z*, and other settings were listed in the Table 1.

2.6. Data processing

All data were analyzed by MetabolitePilot software (AB Sciex, Foster City, CA, USA), blank plasma and brain sample were selected as background control. The metabolites were automatically matched by the software.

Table 1
Mass setting condition.

Ion mode	ESI (+)	ESI (−)
Sheath gas	310 000 Pa	310 000 Pa
Auxiliary gas	310 000 Pa	310 000 Pa
Curtain gas	241 000 Pa	241 000 Pa
Temperature	500 °C	500 °C
Ionspray voltage floating	5 500 V	−4 500 V
Declustering potential	50 V	−50 V
Collision energy	35 V	−35 V
Collision energy scatter (CES)	15 V	15 V

3. Results and discussion

3.1. Identification of chemical constituents within MGD

In order to characterize the chemical constructure of constituents in MGD, UPLC-Q-TOF-MS technique was used, and the representative base peak chromatograms (BPC) of MGD both in negative and positive ion modes were shown in Fig. 1. As a result, a total of 105 components were identified, and 10 of them were verified by chemical standard markers, including gallic acid, protocatechuic acid, coumarin, *trans*-cinnamic acid, syringaldehyde, catechin, epicatechin, ephedrine, pseudoephedrine and (−)-*N*-methylephedrine. It had been reported that the EH mainly contained alkaloids and flavonoids (Zheng, Mu, Pan, Luan, & Zhao, 2023), while phenylpropanoids, organic acids, coumarins and flavonoids were the representative compounds in CR (Zhang et al., 2019). Moreover, a part of the same flavonoids could be identified in both herbs. In our research, we further classified the 105 compounds according to their structures and sources, among which 58 were from EH and 37 from CR (Table 2 and 3).

Flavonoids could exist in both EH and CR, with the potential effect on anti-oxidant, anti-cancer, anti-inflammatory and anti-bacterial (Serafini, Peluso, & Raguzzini, 2010; Tang et al., 2023). In terms of the nucleus structure, flavonoids could be mainly divided into flavone, flavonol, flavanone. Generally, the fragment pattern of flavonoids being representative by catechin in negative ion spectrum could be concluded as followed. Firstly, the quasi-molecular ion *m*/*z* 289.071 8 $[M-H]^-$ of catechin could be observed. Then the diagnostic ions *m*/*z* 137, 151, 179 and 109 could be obtained by retro Diels-Alder (RDA) cleavage, and the *m*/*z* 151 could be further produced the fragment *m*/*z* 123 with losing 28 (CO). Meanwhile, the nucleus structure could lose C_2H_4O or C_3O_2 directly, producing ion fragments *m*/*z* 245 and 221, and the later one could be further eliminated 18 (H_2O), resulting in fragment *m*/*z* 203 being identified. The representative flavonoids catechin in MGD is a flavanol, and the neutral loss 44 of carbonyl on circle C was absent (Fig. S1).

Flavone glycosides are complexes of flavonoid nucleus structure and glycosyls. The glycosidic bonds of the complexes are connected by oxygen or carbon, leading to two different types of flavone glycosides, *O*-glycosides and *C*-glycosides (Abrankó, García-Reyes, & Molina-Díaz, 2011). Bonding by *O*-glycosides, glycosyl is apt to be eliminated first, specifically glucose (162), rhamnose (146) and glucuronic acid (176). The potential fragmentation pathway of quercetin 3-*O*-rhamnoside-7-*O*-glucoside was presented in Fig. S2. It is a one type of di-*O*-glycosides in MGD, and the labeling ions *m*/*z* 463, 447 and 301 were produced by homolysis and heterolysis cleavage of flavone glycosides from quasimolecular ion *m*/*z* 609.146 1, while *m*/*z* 462, 300 and 299 were induced by the radicals from homolytic cleavage. Quercetin 3-*O*-rhamnoside-7-*O*-glucoside was accompanied with the flavonoid diagnosed ion *m*/*z* 272, 271 and 255. Compared to *O*-glycosides, the mass frag-

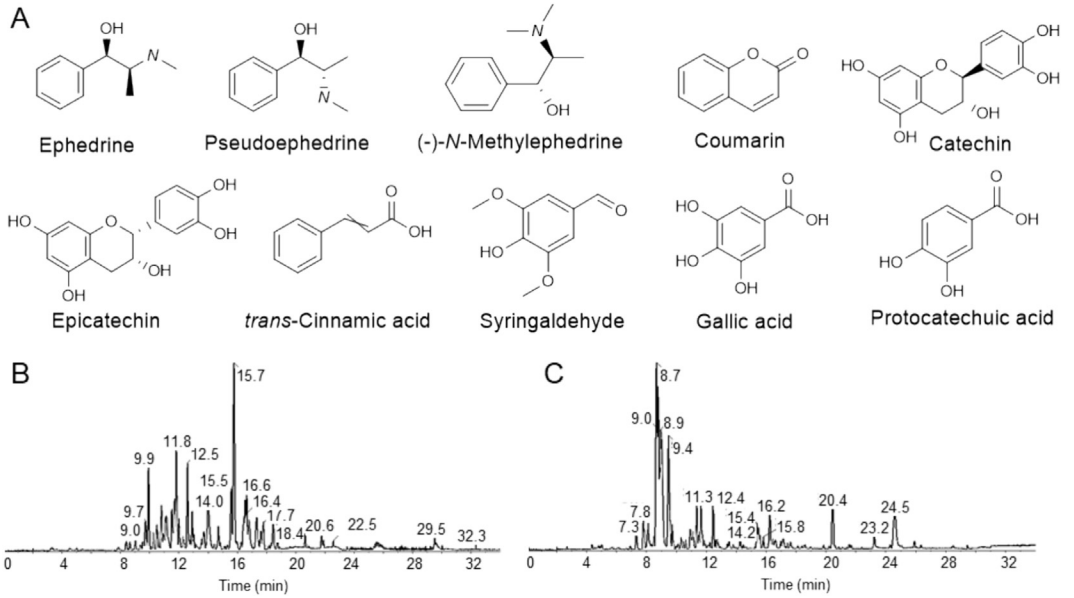

Fig. 1. Representative components and BPC chromatograms of MGD. (A) Typical components in MGD; (B) Negative BPC chromograph; (C) Positive BPC chromograph.

Table 2
Chemical compounds in MGD and their source.

Sources	Alkaloid	Flavonoid	Phenylpropanoid	Organic acid	Glycoside	Amino acid	Coumarin	Others	Total
EH	15	31	–	1	–	8	–	3	58
CR	–	6	16	7	2	–	2	4	37
Uncategorized	–	–	–	–	13	–	–	5	17
Total (Remove duplicates)	15	31	16	8	15	8	2	10	105

EH: *Ephedrae Herba*; CR: *Cinnamomi Ramulus*; –: no detection.

Table 3
Identification of MGD and mass informations.

No.	Identity	Formula	t_R (min)	Ion mode	Cal m/z	m/z	Error	Fragments	Ion mode	Cal m/z	m/z	Error	Fragments	Class	Source
1	Adenine	$C_5H_5N_5$	2.69	$[M-H]^-$	134.047 2	134.047 2	−0.4	134, 107, 65	$[M+H]^+$	136.061 8	136.061 6	−1.5	136, 119, 109, 92, 77, 67, 65	Purine	EH/CR
2	*N*-Acetyl-6-oxo-*L*-norleucine	$C_8H_{13}NO_4$	2.71	–	–	–	–	–	$[M+H]^+$	188.091 7	188.091 5	−1.1	188, 142, 114, 110, 96	Amino acid	EH
3	Citric acid	$C_6H_8O_7$	3.3	$[M-H]^-$	191.019 7	191.019 7	−0.3	111, 87, 85	–	–	–	–	–	Organic acid	EH
4	Adenosine	$C_{10}H_{13}N_5O_4$	4.37	–	–	–	–	–	$[M+H]^+$	268.104 0	268.103 9	−0.5	136, 119	Purine	EH/CR
5	Crotonoside	$C_{10}H_{13}N_5O_5$	4.73	$[M-H]^-$	282.084 4	282.084 3	−0.5	150, 133, 108	$[M+H]^+$	284.098 9	284.098 7	−0.8	152, 135, 110	Purine	EH
6	4-Amino-*L*-phenylalanine	$C_9H_{12}N_2O_2$	5.63	–	–	–	–	–	$[M+H]^+$	181.097 2	181.096 9	−1.7	181, 137, 120, 110, 94	Amino acid	EH
7	Gallic acid*	$C_7H_6O_5$	5.64	$[M-H]^-$	169.014 2	169.014 2	−0.2	125, 79	$[M+H]^+$	171.028 6	171.028 8	−1.2	153, 135, 127, 125, 107, 81, 79, 69, 53	Gallic acid	CR
8	OH-Ephedrine	$C_{10}H_{15}NO_2$	5.69	–	–	–	–	–	$[M+H]^+$	182.117 6	182.117 1	−2.7	164, 146, 134, 119, 118, 105, 91	Alkaloid	EH
9	*OH-Ephedrine*	$C_{10}H_{15}NO_2$	6.09	–	–	–	–	–	$[M+H]^+$	182.117 6	182.117 4	−1.1	164, 146, 134, 119, 118, 105, 91	Alkaloid	EH
10	Phenylalanine	$C_9H_{11}NO_2$	6.22	$[M-H]^-$	164.071 7	164.071 6	−0.6	147, 103, 72	$[M+H]^+$	166.086 3	166.086	−1.8	166, 120, 103, 93, 91	Amino acid	EH
11	2-[[6-(3,4-Dimethylanilino)-4,5-dihydroxy-2-(hydroxymethyl)oxan-3-yl]methoxymethyl]-6-(hydroxymethyl)oxane-3,4,5-triol	$C_{22}H_{35}NO_{10}$	6.93	–	–	–	–	–	$[M+H]^+$	474.233 4	474.233	−0.8	166, 145, 121, 85	Glycoside	–
12	Norephedrine	$C_9H_{13}NO$	7.33	–	–	–	–	–	$[M+H]^+$	152.107 0	152.106 8	−1.2	134, 117, 115, 91, 65	Alkaloid	EH
13	Norpseudoephedrine	$C_9H_{13}NO$	7.8	–	–	–	–	–	$[M+H]^+$	152.107 0	152.106 8	−1.2	134, 117, 115, 91, 65	Alkaloid	EH
14	Sesbanimide C	$C_{15}H_{23}NO_6$	8.11	$[M-H]^-$	312.145 3	312.145 1	−0.6	150, 71, 59	$[M+H]^+$	314.159 8	314.159 7	−0.4	278, 176, 134, 117, 115	Alkaloid	EH
15	Gallocatechin	$C_{15}H_{14}O_7$	8.36	$[M-H]^-$	305.066 7	305.066 5	−0.5	305, 261, 219, 167, 165, 125	$[M+H]^+$	307.081 2	307.081 5	0.9	177, 163, 139	Flavonoid	EH
16	Ephedrine*	$C_{10}H_{15}NO$	8.7	–	–	–	–	–	$[M+H]^+$	166.122 6	166.122 5	−0.8	148, 133, 132, 130, 117, 115, 104, 91, 77, 70, 65, 57, 56	Alkaloid	EH
17	Protocatechuic acid*	$C_7H_6O_4$	8.87	$[M-H]^-$	153.019 3	153.019 2	−0.9	109, 108, 91, 81, 65, 53	–	–	–	–	–	Phenylpropanoid	CR
18	Pseudoephedrine*	$C_{10}H_{15}NO$	8.98	–	–	–	–	–	$[M+H]^+$	166.122 6	166.122 5	−0.8	148, 133, 132, 130, 117, 115, 104, 91, 77, 70, 65, 57, 56	Alkaloid	EH
19	NA	$C_{34}H_{40}O_{18}$	9.21	$[M-H]^-$	735.214 2	735.213 6	−0.8	735, 691, 603, 583, 423, 379	–	–	–	–	–	–	–
20	Ephedradine A	$C_{28}H_{36}N_4O_4$	9.36	–	–	–	–	–	$[M+H]^+$	493.280 9	493.281 4	1.0	493, 464, 348, 265, 155	Alkaloid	EH
21	(−)-*N*-Methylephedrine*	$C_{11}H_{17}NO$	9.47	–	–	–	–	–	$[M+H]^+$	180.138 3	180.138 1	−1.1	180, 162, 147, 146, 132, 117, 115, 91, 77, 65, 57	Alkaloid	EH
22	4-[[3-Cyclopentyloxy-4-(hydroxymethoxyperoxy)-5-	$C_{18}H_{29}NO_9$	9.51	$[M-H]^-$	402.177	402.176 4	−1.4	247, 154, 110	$[M+H]^+$	404.191 5	404.191 8	0.7	336, 318, 300, 282, 216, 174,	Alkaloid	EH

(*continued on next page*)

Table 3 (*continued*)

No.	Identity	Formula	t_R (min)	Ion mode	Cal *m*/*z*	*m*/*z*	Error	Fragments	Ion mode	Cal *m*/*z*	*m*/*z*	Error	Fragments	Class	Source
	methylcyclohex-3-en-1-yl]methyl]-3,3,4-trihydroxypyrrolidin-2-one												114		
23	Isosyringinoside or its isomer	$C_{23}H_{34}O_{14}$	9.59	$[M + FA-H]^-$	579.193 1	579.192 1	−1.7	371, 209, 179, 161, 119, 89	–	–	–	–	–	Phenylpropanoid	CR
24	NA	$C_{13}H_{18}N_4O_3$	9.71	$[M-H]^-$	277.130 6	277.130 2	−1.5	277, 235, 191, 120	$[M + H]^+$	279.145 2	279.145 5	1.2	279, 262, 220, 219, 201, 176	Alkaloid	EH
25	Prenyl glucoside	$C_{11}H_{20}O_6$	9.73	–	–	–	–	–	$[M + NH_4]^+$	266.159 8	266.159 3	−1.9	163, 145, 127, 85, 69	Glycoside	CR
26	Feruloylhistamine	$C_{15}H_{17}N_3O_3$	10.19	–	–	–	–	–	$[M + H]^+$	288.134 3	288.135	2.5	288, 177, 145, 141, 117, 112	Amino acid	EH
27	1-(3-Methylbutanoyl)-6-apiosylglucose	$C_{16}H_{28}O_{11}$	10.26	$[M-H]^-$	395.155 9	395.155 4	−1.2	395, 293, 251, 161, 125, 101, 99	$[M + H]^+$	397.170 4	397.170 7	0.7	145, 127, 103, 85	Glycoside	–
28	Syringin	$C_{17}H_{24}O_9$	10.32	–	–	–	–	–	$[M + NH_4]^+$	390.175 9	390.175 5	−1.0	211, 193, 161, 133	Phenylpropanoid	CR
29	Epigallocatechin	$C_{15}H_{14}O_7$	10.36	$[M-H]^-$	305.066 7	305.066 5	−0.5	305, 261, 219, 167, 165, 125	$[M + H]^+$	307.081 2	307.081 5	0.9	177, 163, 139	Flavonoid	EH
30	Isovitexin-7-*O*-glucosyl-2′′*O*-rhamnoside	$C_{33}H_{40}O_{19}$	10.59	$[M-H]^-$	739.203 2	739.203	−0.3	739, 649, 619, 587, 449, 287, 167	$[M + H]^+$	741.223 7	741.224 4	0.9	741, 595, 577, 559, 529, 475, 445, 415, 397, 367, 337, 313, 283	Flavonoid	EH
31	Catechin*	$C_{15}H_{14}O_6$	10.64	$[M-H]^-$	289.071 8	289.071 5	−0.9	289, 245, 203, 137, 125, 109	$[M + H]^+$	291.086 3	291.086	−1.1	289, 245, 203, 151, 123, 109, 97	Flavonoid	EH/CR
32	*p*-Coumaric acid glucoside	$C_{15}H_{18}O_8$	10.65	$[M-H]^-$	325.092 9	325.092 9	0	163, 119	–	–	–	–	–	Phenylpropanoid	CR
33	11-[(2*S*,3*S*,4*S*,5*R*,6*R*)-3,5-Dihydroxy-4-[(2*S*,3*S*,4*S*,5*S*,6*R*)-3,4,5-trihydroxy-6-(hydroxymethyl)oxan-2-yl]oxy-6-[[(2*S*,3*S*,4*S*,5*S*,6*R*)-3,4,5-trihydroxy-6-(hydroxymethyl)oxan-2-yl]oxymethyl]oxan-2-yl]oxyundecane-3,8-dione	$C_{29}H_{50}O_{18}$	10.67	$[M + COOH-H]^-$	731.297 9	731.296 6	−1.8	685, 523, 361, 221, 99	–	–	–	–	–	Glycoside	–
34	Ephedrannin Tr1	$C_{45}H_{36}O_{21}$	10.72	$[M-H]^-$	911.167 6	911.167 5	−0.1	911, 865, 743, 607, 305	–	–	–	–	–	Flavonoid	EH
35	Ephedrannin *D*4/*D*5/*D*6/*D*7	$C_{30}H_{24}O_{14}$	10.81	$[M-H]^-$	607.109 3	607.109 2	−0.1	607, 571, 481, 439, 305, 301	$[M + H]^+$	609.123 9	609.124 3	0.7	441, 303	Flavonoid	EH
36	Ephedrannin Tr2	$C_{45}H_{36}O_{20}$	10.82	$[M-H]^-$	895.172 7	895.172 8	0.1	895, 727, 594, 427, 349	$[M + H]^+$	897.187 3	897.188 1	0.9	897, 729, 607, 593, 441, 303	Flavonoid	EH
37	CO_2-Phthaloyl leucine	$C_{21}H_{28}N_2O_8$	10.99	$[M-H]^-$	435.177 3	435.177	−0.6	280, 262, 234, 129	$[M + H]^+$	437.191 8	437.191 6	−0.5	437, 264, 246, 200, 134, 117	Amino acid	EH
38	6,8-Di-*C*-hexosyl apigenin	$C_{27}H_{30}O_{15}$	11.11	$[M-H]^-$	593.151 2	593.150 7	−0.9	593, 503, 473, 413, 383, 353	$[M + H]^+$	595.165 8	595.165 2	−0.9	595, 577, 559, 541, 529, 523, 511, 499, 481, 457, 439, 409, 379, 355, 337, 325, 295	Flavonoid	EH
39	Procyanidin B1	$C_{30}H_{26}O_{12}$	11.16	$[M-H]^-$	577.135 1	577.134 8	−0.6	577, 425, 407, 289, 245, 203, 161, 125	$[M + H]^+$	579.149 7	579.149 5	−0.4	579, 427, 409, 301, 287, 275, 247, 233, 191, 163, 139, 127	Flavonoid	EH
40	Benzyl *B*-primeveroside	$C_{18}H_{26}O_{10}$	11.22	$[M-H]^-$	401.145 3	401.145 1	−0.5	401, 269, 233, 161, 113	–	–	–	–	–	Glycoside	CR
41	*N*-Benzoylaspartic acid	$C_{11}H_{11}NO_5$	11.29	$[M-H]^-$	236.056 3	236.056 4	−0.6	236, 192, 120, 77	$[M + H]^+$	238.071	238.070 6	−1.7	105, 77	Amino acid	EH

Table 3 (*continued*)

No.	Identity	Formula	t_R (min)	Ion mode	Cal *m*/*z*	*m*/*z*	Error	Fragments	Ion mode	Cal *m*/*z*	*m*/*z*	Error	Fragments	Class	Source
42	Phthaloyl leucine	$C_{20}H_{28}N_2O_6$	11.3	–	–	–	–	–	$[M + H]^+$	393.202	393.202	0.0	393, 264, 246, 200, 134, 117	Amino acid	EH
43	Tomentin 6,4′-diglucoside	$C_{29}H_{34}O_{18}$	11.31	$[M-H]^-$	669.167 2	669.167 4	0.3	669, 507, 345	$[M + H]^+$	671.181 8	671.182 6	1.2	671, 509, 347	Flavonoid	EH
44	Eugenyl glucoside	$C_{16}H_{22}O_7$	11.36	–	–	–	–	–	$[M + NH_4]^+$	344.170 4	344.17	−1.2	165, 107, 85	Glycoside	–
45	Dihydrocinnacasside or its isomer	$C_{15}H_{20}O_8$	11.46	$[M-H]^-$	327.108 5	327.108 3	−0.7	257, 147, 113, 103, 89, 71, 59	–	–	–	–	–	Phenylpropanoid	CR
46	Epicatechin*	$C_{15}H_{14}O_6$	11.52	$[M-H]^-$	289.071 8	289.071 5	−0.9	289, 245, 203, 137, 125, 109	$[M + H]^+$	291.086 3	291.086	−1.1	289, 245, 203, 151, 123, 109, 97	Flavonoid	EH/CR
47	Schaftoside	$C_{26}H_{28}O_{14}$	11.53	$[M-H]^-$	563.140 6	563.140 3	−0.6	563, 503, 473, 443, 383, 353	$[M + H]^+$	565.155 2	565.154 8	−0.7	565, 547, 529, 511, 481, 457, 427, 379, 349, 325, 295	Flavonoid	EH
48	Dihydroroseoside	$C_{19}H_{32}O_8$	11.59	$[M + COOH-H]^-$	433.207 9	433.207 2	−1.7	387, 372, 255, 153, 161, 119	$[M + H]^+$	389.217	389.216 7	−0.8	227, 209, 191, 149, 125	Glycoside	–
49	NA	$C_{18}H_{24}O_{11}$	11.59	$[M-H]^-$	415.124 6	415.124 1	−1.2	415, 269, 161, 101, 87	–	–	–	–	–	–	–
50	Isoschaftoside	$C_{26}H_{28}O_{14}$	11.72	$[M-H]^-$	563.140 6	563.140 6	0	563, 503, 473, 443, 383, 353	$[M + H]^+$	565.155 2	565.154 8	−0.7	565, 547, 529, 511, 481, 457, 427, 379, 349, 325, 295	Flavonoid	EH
51	18S-Cinncassiol A 19-*O*-*β*-*D*-glucopyranoside	$C_{26}H_{40}O_{12}$	11.73	$[M-H]^-$	543.244 7	543.244 5	−0.4	543, 363, 167	$[M + H]^+$	562.285 8	562.286	0.4	383, 365, 317, 299	Phenylpropanoid	CR
52	Ephedrannin *D*1/*D*2/*D*3	$C_{30}H_{24}O_{13}$	11.75/ 12.08/ 12.60	$[M-H]^-$	591.114 4	59.114 4	−0.1	591, 555, 465, 407, 301, 289, 175	$[M + H]^+$	593.129 0	593.129 4	0.7	453, 441, 303, 123	Flavonoid	EH
53	Ephedrine derivative	$C_{14}H_{19}NO_5$	11.79	$[M-H]^-$	280.119	280.118 8	−0.9	280, 262, 234, 218, 156	$[M + H]^+$	282.133 6	282.133 2	−1.4	134, 117	Alkaloid	EH
54	NA	$C_{14}H_{12}N_2O_5$	12.00	$[M-H]^-$	287.067 3	287.067	−1.2	287, 243, 215, 183, 173, 145, 96	–	–	–	–	–	–	–
55	*O*-Coumaric acid glucoside	$C_{15}H_{18}O_8$	12.08	$[M-H]^-$	325.092 9	325.092 7	−0.6	163, 119	–	–	–	–	–	Phenylpropanoid	CR
56	Perilloside B	$C_{16}H_{24}O_7$	12.08	$[M-H]^-$	327.144 9	327.144 6	−1	327, 165	$[M + NH_4]^+$	346.186	346.186	0.0	173, 149, 127, 107, 85	Glycoside	–
57	Quercetin 3-*O*-rhamnoside-7-*O*-glucoside	$C_{27}H_{30}O_{16}$	12.14	$[M-H]^-$	609.146 1	609.146	−0.2	609, 463, 447, 300, 299, 271	$[M + H]^+$	611.160 7	611.161 2	0.9	465, 303	Flavonoid	EH/CR
58	Lyoniresinol 9′-*O*-glucoside	$C_{28}H_{38}O_{13}$	12.3	$[M-H]^-$	581.224	581.223	−1.7	581, 419, 371, 223, 195	–	–	–	–	–	Glycoside	–
59	7-Caffeoylsedoheptulose	$C_{16}H_{20}O_{10}$	12.3	$[M-H]^-$	371.098 4	371.098	−1	371, 249, 231, 121	$[M + H]^+$	373.112 9	373.113	0.1	179, 105	Phenylpropanoid	CR
60	Vitexin	$C_{21}H_{20}O_{10}$	12.46	$[M-H]^-$	431.098 4	431.098 2	−0.4	431, 341, 311, 283, 281, 269	$[M + H]^+$	433.112 9	433.113 1	0.4	433, 415, 397, 379, 367, 337, 313, 283	Flavonoid	EH
61	Vitexin-2-*O*-rhamnoside	$C_{27}H_{30}O_{14}$	12.46	$[M-H]^-$	577.156 3	577.156 1	−0.3	577, 457, 413, 323, 293	$[M + H]^+$	579.170 8	579.170 4	−0.7	433, 415, 397, 379, 367, 337, 313, 383	Flavonoid	EH
62	(Epi) afzelechin	$C_{15}H_{14}O_5$	12.56	$[M-H]^-$	273.076 8	273.076 7	−0.4	273, 205, 189, 137, 93	$[M + H]^+$	275.091 4	275.091 1	−1.1	149, 145, 139, 107	Flavonoid	EH
63	Ephedrine derivative	$C_{13}H_{17}NO_4$	12.73	$[M-H]^-$	250.108 5	250.108 4	−0.3	128, 98	$[M + H]^+$	252.123	252.122 9	−0.5	134, 117, 101, 91, 73	Alkaloid	EH
64	5-Hydroxyferulic acid	$C_{10}H_{10}O_5$	12.73	$[M-H]^-$	209.045 5	209.045 6	0.3	165, 121, 120, 77, 76	–	–	–	–	–	Phenylpropanoid	CR
65	10-*O*-Acetylgeniposide	$C_{19}H_{26}O_{11}$	12.74	$[M-H]^-$	429.140 2	429.139 9	−0.8	429, 383, 119, 87	–	–	–	–	–	Glycoside	–

(*continued on next page*)

Table 3 (*continued*)

No.	Identity	Formula	t_R (min)	Ion mode	Cal *m/z*	*m/z*	Error	Fragments	Ion mode	Cal *m/z*	*m/z*	Error	Fragments	Class	Source
66	Isovitexin	$C_{21}H_{20}O_{10}$	12.75	$[M-H]^-$	431.098 4	431.098 2	−0.4	431, 341, 311, 283, 281, 269	$[M + H]^+$	433.112 9	433.113 1	0.4	433, 415, 397, 379, 367, 337, 313, 283	Flavonoid	EH
67	3,6-Diglucopyranosyl-5,7-dihydroxy-4′-methoxyflavone	$C_{28}H_{32}O_{15}$	12.79	$[M-H]^-$	607.166 8	607.166	−1.4	607, 487, 443, 323	$[M + H]^+$	609.181 4	609.181 9	0.8	609, 463, 445, 427, 367, 343, 313	Flavonoid	EH
68	Buddlenol *C*-2Glc	$C_{44}H_{58}O_{22}$	12.81	$[M + COOH-H]^-$	983.340 2	983.34	−0.2	937, 775, 613, 565, 417, 387, 195	–	–	–	–	–	Phenylpropanoid	CR
69	Proanthocyanidin A1	$C_{30}H_{24}O_{12}$	12.9	$[M + COOH-H]^-$	621.125	621.124 9	−0.1	575, 557, 539, 452, 423, 289, 285, 163	$[M + H]^+$	577.134 1	577.134 4	0.7	425, 287	Flavonoid	EH
70	Diethyl 2,5-dihydroxyterephthalate	$C_{12}H_{14}O_6$	13.21	–	–	–	–	–	$[M + H]^+$	255.086 3	255.086 1	−0.9	193, 149, 121, 65	Phthalate	–
71	Quercetin 3-(2-glucosylrhamnoside)	$C_{27}H_{30}O_{16}$	13.23	$[M-H]^-$	609.146 1	609.146 1	−0.2	609, 445, 301, 300	$[M + H]^+$	611.160 7	611.161	0.5	465, 303	Flavonoid	EH/CR
72	Proanthocyanidin A2	$C_{30}H_{24}O_{12}$	13.48	$[M + COOH-H]^-$	621.125	621.124 9	−0.1	575, 557, 539, 452, 423, 289, 285, 163	$[M + H]^+$	577.134 1	577.134 4	0.7	425, 287	Flavonoid	EH
73	6‴-(3-Hydroxy-3-methylglutaroyl) isoviolanthin	$C_{33}H_{38}O_{18}$	13.51	$[M-H]^-$	721.198 5	721.198 7	0.2	721, 659, 619, 577, 559, 457, 413, 293, 161	$[M + H]^+$	723.213 1	723.212 6	−0.7	723, 577, 559, 541, 379, 307, 313	Flavonoid	EH
74	Isorhamnetin-3-*O*-glucoside	$C_{22}H_{22}O_{12}$	13.54	$[M-H]^-$	477.103 8	477.103 6	−0.5	477, 315, 314, 300, 299, 271, 255	$[M + H]^+$	479.118 4	479.118 2	0.7	449, 413, 345, 303, 261, 225	Flavonoid	EH
75	*N*-(3-Indolylacetyl)-*DL*-aspartic acid	$C_{14}H_{14}N_2O_5$	13.54	$[M-H]^-$	289.083	289.082 9	−0.4	245, 203, 159, 116, 74	$[M + H]^+$	291.097 5	291.097 5	0.0	245, 227, 185, 159, 142, 130	Amino acid	EH
76	Quercetin-3-*D*-galactoside	$C_{21}H_{20}O_{12}$	13.55	$[M-H]^-$	463.088 2	463.088 1	−0.3	301, 255	$[M + H]^+$	465.102 8	465.103	0.5	303	Flavonoid	EH/CR
77	Syringaldehyde*	$C_9H_{10}O_4$	13.59	$[M-H]^-$	181.050 6	181.050 6	−0.7	166, 151, 123, 95, 90, 79, 67, 61	–	–	–	–	–	Phenols	CR
78	Quercetin 3-*O*-alpha-*L*-rhamnopyranosyl-(1->2)-alpha-*L*-arabinopyranoside	$C_{26}H_{28}O_{15}$	13.7	$[M-H]^-$	579.135 5	579.135 3	0.4	579, 417, 300, 245, 203, 181	$[M + H]^+$	581.150 1	581.150 5	0.9	449, 413, 345, 303	Flavonoid	EH/CR
79	2-*O*-Feruloyltartronic acid	$C_{13}H_{12}O_8$	13.97	$[M-H]^-$	295.045 9	295.045 5	−1.5	173, 154, 111, 85, 67	$[M + NH_4]^+$	314.087	314.087 1	0.2	123, 105, 79, 77	Phenylpropanoid	CR
80	Mahuannin A/B/C	$C_{30}H_{24}O_{10}$	14.03/ 14.38/ 14.59	$[M-H]^-$	543.129 7	543.129 7	0.1	543, 417, 301, 273, 241, 153	$[M + H]^+$	545.144 2	545.144 6	0.7	509, 409, 391, 271, 255, 243, 215	Flavonoid	EH
81	Loliolide	$C_{11}H_{16}O_3$	14.27	–	–	–	–	–	$[M + H]^+$	197.117 2	197.116 8	−2.0	197, 179, 161, 133, 107, 105, 91	Benzofurans	–
82	Kaempferol 3-xylosyl-(1->2)-rhamnoside	$C_{26}H_{28}O_{14}$	14.38	$[M-H]^-$	563.140 6	563.140 1	−0.9	563, 431, 284, 255, 227	–	–	–	–	–	Flavonoid	EH
83	3-(2-Hydroxyphenyl)propanoic acid	$C_9H_{10}O_3$	14.41	$[M-H]^-$	165.055 7	165.055 6	−0.5	121, 106	–	–	–	–	–	Phenylpropanoid	CR
84	Kaempferol rhamnoside	$C_{21}H_{20}O_{10}$	14.57	$[M-H]^-$	431.098 4	431.098 4	0	431, 285, 284, 255, 227	$[M + H]^+$	433.112 9	433.113 2	0.6	287, 165, 85, 71	Flavonoid	EH
85	*Ephedrine derivative*	$C_{12}H_{17}NO_2$	14.61	–	–	–	–	–	$[M + H]^+$	208.133 2	208.133	−1.0	190, 148, 133, 117, 91	Alkaloid	EH
86	Semiaquilinoside	$C_{28}H_{32}O_{14}$	14.62	$[M-H]^-$	591.171 9	591.171 6	−0.6	591, 471, 445, 355, 325, 307, 119	$[M + H]^+$	593.186 5	593.186 2	−0.5	593, 447, 429, 411, 393, 381, 351, 327, 297	Flavonoid	EH
87	*N*-Methyl-*N*-[2-[4-[3-*O*-[4-*O*-(alpha-*L*-rhamnopyranosyl)-6-*O*-benzoyl-beta-*D*-glucopyranosyl]-alpha-*L*-	$C_{36}H_{49}NO_{16}$	14.62	–	–	–	–	–	$[M + H]^+$	752.312 4	752.312 1	−0.4	606, 340, 194, 121	Glycoside	–

Table 3 (*continued*)

No.	Identity	Formula	t_R (min)	Ion mode	Cal *m*/*z*	*m*/*z*	Error	Fragments	Ion mode	Cal *m*/*z*	*m*/*z*	Error	Fragments	Class	Source
	rhamnopyranosyloxy]phenyl]ethyl] acetamide														
88	Azelaic acid	$C_9H_{16}O_4$	14.69	$[M-H]^-$	187.097 6	187.097 4	−1	187, 125, 123, 97	–	–	–	–	–	Organic acid	CR
89	4-Hydroxycinnamic acid	$C_9H_8O_3$	14.76	$[M-H]^-$	163.040 1	163.04	−0.4	119, 117, 93	–	–	–	–	–	Phenylpropanoid	CR
90	*N*-Methyl-*N*-[2-[4-[3-*O*-[4-*O*-(alpha-*L*-rhamnopyranosyl)-6-*O*-[(*E*)-3-phenyl-1-oxo-2-propenyl]-*β*-*D*-glucopyranosyl]-alpha-*L*-rhamnopyranosyloxy]phenyl]ethyl] acetamide	$C_{38}H_{51}NO_{16}$	15.23	–	–	–	–	–	$[M+H]^+$	778.328 1	778.329	1.2	632, 340, 194, 131	Alkaloid	EH
91	5-Methyl-2-(1-methylethyl)phenyl	$C_{16}H_{24}O_6$	15.54	$[M+COOH-H]^-$	357.155 5	357.155 1	−1.1	311, 161, 101, 85	$[M+NH_4]^+$	330.191 1	330.191 1	0	133, 105	Glycoside	–
92	*β*-*D*-Glucosyl-1-amidophyllantocin	$C_{30}H_{39}NO_{11}$	15.55	$[M+COOH-H]^-$	634.250 5	634.250 1	−0.7	307, 280, 161, 145	$[M+H]^+$	590.259 6	590.259 7	0.2	428, 298, 282, 152, 131	Phenylpropanoid	CR
93	Sydowic acid	$C_{15}H_{20}O_4$	15.56	$[M-H]^-$	263.128 9	263.128 8	−0.2	219, 204, 189, 153, 136, 122	$[M+H]^+$	265.143 7	265.143 4	−1.1	247, 201, 187, 173, 159, 135, 121	Organic acid	CR
94	Geranyl beta-*D*-glucopyranoside	$C_{16}H_{28}O_6$	15.75	$[M+COOH-H]^-$	361.186 8	361.186 4	−1.1	361, 315, 161, 113, 101	$[M+NH_4]^+$	334.222 4	334.222	−1.2	137, 81	Glycoside	–
95	Coumarin*	$C_9H_6O_2$	15.82	–	–	–	–	–	$[M+H]^+$	147.044 1	147.043 9	−1.4	147, 103, 91, 77, 65	Coumarin	CR
96	Malonic acid 1-[1-*O*-(2-methyl-5-isopropylphenyl)-6-deoxy-beta-*D*-glucopyranose-6-Yl]ester	$C_{19}H_{26}O_9$	16.23	–	–	–	–	–	$[M+NH_4]^+$	416.191 5	416.191 8	0.7	133, 106	Glycoside	–
97	*D*-Linalool 3-(6′′-malonylglucoside)	$C_{19}H_{30}O_9$	16.31	–	–	–	–	–	$[M+NH_4]^+$	420.222 8	420.223 2	1.0	249, 231, 145, 137, 127, 105, 81	Glycoside	–
98	*trans*-Cinnamic acid*	$C_9H_8O_2$	16.53	$[M-H]^-$	147.045 2	147.045 1	−0.5	103, 77	$[M+H]^+$	149.059 7	149.059 4	−2.1	131, 103, 77	Phenylpropanoid	CR
99	9,12,13,TriHODE	$C_{18}H_{32}O_5$	16.76	$[M-H]^-$	327.217 7	327.217 2	−1.5	327, 291, 239, 229, 211, 183, 171	$[M+NH_4]^+$	346.258 8	346.258 5	−0.9	293, 275, 195, 155	Organic acid	CR
100	7-Methylcoumarin	$C_{10}H_8O_2$	17.04	–	–	–	–	–	$[M+H]^+$	161.059 7	161.059 5	−1.2	146, 118, 91, 89, 77	Coumarin	CR
101	Pinellic acid	$C_{18}H_{34}O_5$	17.31	$[M-H]^-$	329.233 3	329.233 1	−0.8	329, 229, 211, 183, 171, 139	–	–	–	–	–	Organic acid	CR
102	16-Hydroxy-10-oxohexadecanoic acid	$C_{16}H_{30}O_4$	17.49	$[M-H]^-$	285.207 1	285.206 9	−0.8	285, 255, 181	–	–	–	–	–	Organic acid	CR
103	2-Methoxycinnamaldehyde	$C_{10}H_{10}O_2$	18.39	–	–	–	–	–	$[M+H]^+$	163.075 4	163.075 1	−1.8	145, 135, 115, 107, 91, 77	Phenylpropanoid	CR
104	Truxillic acid	$C_{18}H_{16}O_4$	18.46	$[M-H]^-$	295.097 6	295.097 3	−0.9	277, 233, 205, 147, 103, 77	–	–	–	–	–	Organic acid	CR
105	13-HPODE(1-)	$C_{18}H_{32}O_4$	19.4	$[M-H]^-$	311.222 8	311.222 5	−1	311, 293, 275, 235, 223, 87	–	–	–	–	–	Organic acid	CR

* Constituents verified by chemical standard regent; –: constituents could not be identified according to detected mass information; EH: *Ephedrae Herba*; CR: *Cinnamomi Ramulus*; NA: no match to the corresponding compound.

ments ions of *C*-glycosides were mainly from carbohydrate chain and the cleavage within the carbon ring of glycosyl, that is, the cleavage at (^{0,2}X), (^{0,3}X) and (^{0,4}X) leading to the neutral loss of $C_4H_8O_4$ (120), and $C_3H_6O_3$ (90) and $C_2H_4O_2$ (60) could be used to identify the *C*-glycosides. The potential pathway of isoschaftoside was presented in Fig. S2.

Flavonoid polymers belonging to EH are special flavonoid in MGD, which were being binding by either two or more flavonoids or polymerized with other chemical structure, and some of them had been proved to possess antimicrobial efficacy (Zang et al., 2013). Ephedrannin Tr1 is polymerized by three flavanols and several gallic acid structures, in its MS^2 spectrum, *m*/*z* 743 was produced from *m*/*z* 911 $[M-H]^-$ owing to the RDA cleavage, following by the loss of 18 (H_2O). Meanwhile the bonding site of flavonoids could be lost directly, leading to the fragmentation ion *m*/*z* 607 and 305 (Fig. S3).

3.2. Identification of alkaloids in MGD

Ephedrine and its isomers, including ephedrine, pseudoephedrine, norephedrine and norpseudoephedrine, are the potential bio-active compounds in EH with the efficiencies on asthma, allergy and cough (Tang et al., 2023). The possible cleavage pathways could be concluded in Fig. S4. Specifically, the parenting ion *m*/*z* 166 $[M + H]^+$ of ephedrine could experience the α cleavage, *i* cleavage and hydrogen rearrangement, leading to the identified ions *m*/*z* 56. The *m*/*z* 166 could also cause the neutral loss of 18 (H_2O), followed by eliminating CH_3 or CH_4N, resulting in *m*/*z* 148, 133, 132 and 115. Meanwhile, we could also identify the diagnosed mass ion *m*/*z* 77 and 91 of benzene ring with a methyl.

3.3. Identification of phenylpropanoids in MGD

The nuclear structure of phenylpropanoids was combined by one or several C_6-C_3 chains, widely existing in various kinds of herbs. Because of their diversity structures, the physiological functions could be different (Vogt, 2010). In CR, phenylpropanoids have shown their benefits on preventing tumor, oxidant and inflammation as well as neuroprotection (Liu et al., 2020). The cleavage of phenylpropanoids usually happened between the C_6-C_3 bonding site or the branched chain. The cleavage pathway isosyringinoside was shown in Fig. S5. There were two glucosides bonding with the C_6-C_3, leading to the successively losing glycosides glucose (162) from 579 $[M + COOH-H]^-$. Meanwhile, the diagnosed mass ions of glucose residuces (*m*/*z* 179, 119 and 85) could be observed.

3.4. Identification of amino acids in MGD

In our study, we also identified amino acids and their derivates in MGD referred from the MS^2 spectrum and the Pubchem database. However, relevant studies about those amino acids in EH or CR were rarely reported. Amino pathway is the main anabolism procedure of ephedra alkaloids (Krizevski et al., 2010), and we therefore speculated that the identified amino acids were mainly from EH.

N-(3-Indolylacetyl)-*DL*-aspartic acid was combined by indole and aspartic acid, and the mass ion *m*/*z* 245, 201 and 227 could be found from its MS^2 spectrum due to the losing of 46 (CHO_2) or 18 (H_2O). Moreover, indole structure could be broken or cracked from *N*-(3-Indolylacetyl)-*DL*-aspartic acid, producing mass ions *m*/*z* 130 and 159 (Fig. S6).

3.5. In vivo studies of MGD

3.5.1. In vivo identification of prototype constituents and metabolites of MGD

The total ion chromatography (TIC) and extracted ion chromatography (XIC) of plasma and brain were shown in Figs. 2 and 3. As for prototype constituents, based on the chemical characterization of MGD (Table 3), including the information of molecular weight, relative intensity of MS^2 fragmentation and retention time in the extracted ion chromatography (XIC) were used to analyze the potential prototype constituents in plasma and brain samples. In accordance with the similar mass and chromatography behavior, 30 corresponding prototype constituents in plasma and 10 in brain were identified (Table 4).

As for the metabolites, depending on the similarity of MS^2 fragment profile and metabolic regulation of phase I and phase II to match them with the corresponding prototype constituents, we used MetabolitePilot software (AB Sciex, Foster City, CA, USA) to screen, identify and mark the metabolites from the samples that were differentiated from the prototype one. Referring to the previous studies, we matched 33 metabolites with their prototypes (Table 5). Some of them could be absorbed into blood directly,

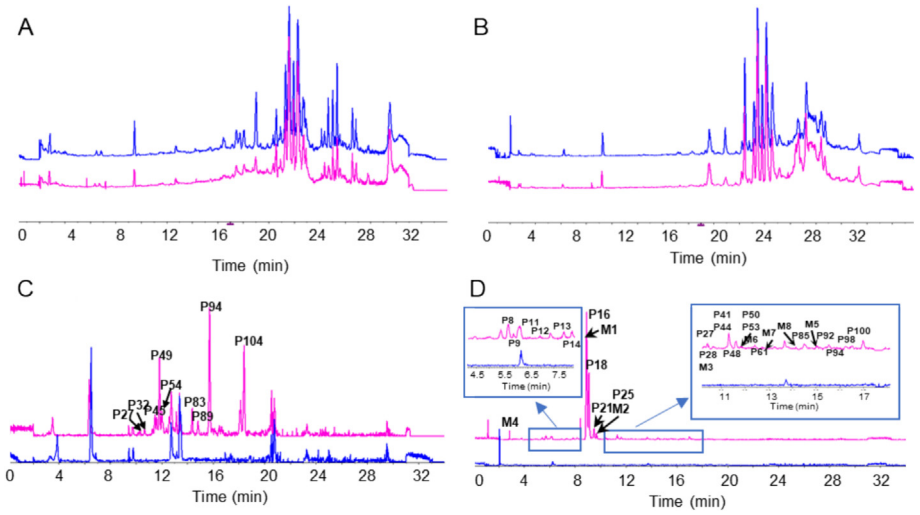

Fig. 2. TIC and XIC of MGD in plasma. (A) Negative TIC chromatogram; (B) Positive TIC chromatogram; (C) Negative XIC chromatogram; (D) Positive XIC chromatogram. All representative chromographs of MGD in plasma were presented after 30 min MGD treatment. Blue line for blank plasma; pink line for MGD treatment plasma.

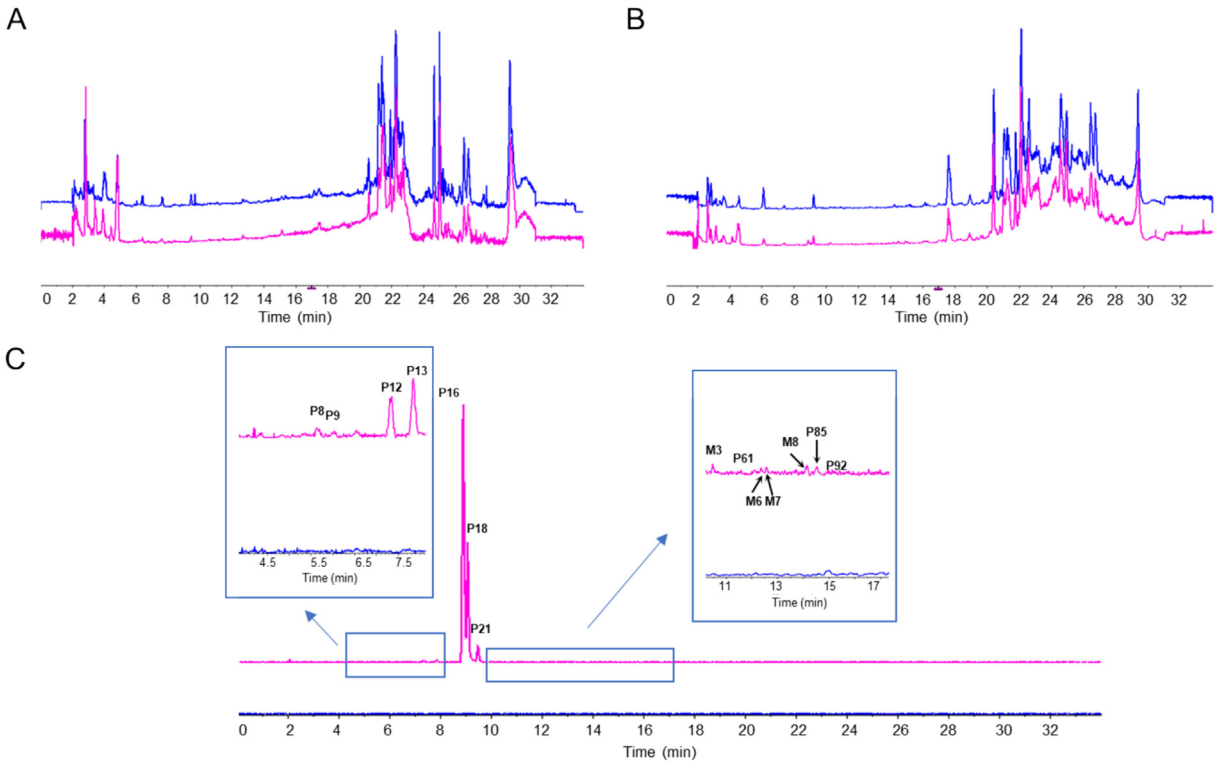

Fig. 3. TIC and XIC of MGD in brain. (A) Negative TIC chromatogram; (B) Positive TIC chromatogram; (C) Positive XIC chromatogram. All representative chromographs of MGD in brain were presented after 60 min MGD treatment. Blue line for blank brain tissue; pink line for MGD treatment brain tissue.

Table 4
Identified prototype constituents in plasma and brain samples.

No.	Name	Formula	t_R (min)	Class	Source	Plasma	Brain
8[#]	OH-Ephedrine	$C_{10}H_{15}NO_2$	5.69	Alkaloid	EH	√	√
9[#]	OH-Ephedrine	$C_{10}H_{15}NO_2$	6.09	Alkaloid	EH	√	√
11	2-[[6-(3,4-Dimethylanilino)-4,5-dihydroxy-2-(hydroxymethyl)oxan-3-yl]methoxymethyl]-6-(hydroxymethyl)oxane-3,4,5-triol	$C_{22}H_{35}NO_{10}$	6.93	Glycoside	–	√	–
12	Norephedrine	$C_9H_{13}NO$	7.33	Alkaloid	EH	√	√
13	Norpseudoephedrine	$C_9H_{13}NO$	7.80	Alkaloid	EH	√	√
14	Sesbanimide C	$C_{15}H_{23}NO_6$	8.11	Alkaloid	EH	√	
16	Ephedrine	$C_{10}H_{15}NO$	8.70	Alkaloid	EH	√	√
18	Pseudoephedrine	$C_{10}H_{15}NO$	8.98	Alkaloid	EH	√	√
21	(−)-*N*-Methylephedrine	$C_{11}H_{17}NO$	9.47	Alkaloid	EH	√	√
25	Prenyl glucoside	$C_{11}H_{20}O_6$	9.73	Glycoside	CR	√	–
27	1-(3-Methylbutanoyl)-6-apiosylglucose	$C_{16}H_{28}O_{11}$	10.26	Glycoside	–	√	–
28	Syringin	$C_{17}H_{24}O_9$	10.32	Phenylpropanoid	CR	√	–
32	*p*-Coumaric acid glucoside	$C_{15}H_{18}O_8$	10.65	Phenylpropanoid	CR	√	–
41	*N*-Benzoylaspartic acid	$C_{11}H_{11}NO_5$	11.29	Amino acid	EH	√	–
44	Eugenyl glucoside	$C_{16}H_{22}O_7$	11.36	Glycoside	–	√	–
45	Dihydrocinnacaside or its isomer	$C_{15}H_{20}O_8$	11.46	Phenylpropanoid	CR	√	–
48	Dihydroroseoside	$C_{19}H_{32}O_8$	11.59	Glycoside	–	√	–
49	NA	$C_{18}H_{24}O_{11}$	11.59	–	–	√	–
50	Isoschaftoside	$C_{26}H_{28}O_{14}$	11.72	Flavonoid	EH	√	–
53	Ephedrine derivative	$C_{14}H_{19}NO_5$	11.79	Alkaloid	EH	√	–
54	NA	$C_{14}H_{12}N_2O_5$	12.00	–	–	√	–
61[#]	Vitexin-2-*O*-rhamnoside	$C_{27}H_{30}O_{14}$	12.46	Flavonoid	EH	√	√
83	3-(2-Hydroxyphenyl)propanoic acid	$C_9H_{10}O_3$	14.41	Phenylpropanoid	CR	√	–
85	*Ephedrine derivative*	$C_{12}H_{17}NO_2$	14.61	Alkaloid	EH	√	√
89	4-Hydroxycinnamic acid	$C_9H_8O_3$	14.76	Phenylpropanoid	CR	√	–
92[#]	*β*-*D*-Glucosyl-1-amidophyllantocin	$C_{30}H_{39}NO_{11}$	15.55	Phenylpropanoid	CR	√	√
94	Geranyl *β*-*D*-glucopyranoside	$C_{16}H_{28}O_6$	15.75	Glycoside	–	√	–
98	*trans*-Cinnamic acid	$C_9H_8O_2$	16.53	Phenylpropanoid	CR	√	–
100	7-Methylcoumarin	$C_{10}H_8O_2$	17.04	Coumarin	CR	√	–
104	Truxillic acid	$C_{18}H_{16}O_4$	18.46	Organic acid	CR	√	–

[#] Constituents had corresponding retention time in brain without further confirmation by MS^2 ion; –: constituents could not be identified according to detected mass information; EH: *Ephedrae Herba*; CR: *Cinnamomi Ramulus*; NA: no match to the corresponding compound.

Table 5
Matching of potential biotransformation.

Prototypes No.	Prototypes name	Metabolites No.	Metabolites name	Biotransformation	Metabolic Formula	*m/z*	Error	t_R (min)	Score (%)
P21	(−)-*N*-Methylephedrine	**M1**	M1	Glucuronidation	$C_{17}H_{25}NO_7$	356.171 1	2.0	8.91	60.4
P21	(−)-*N*-Methylephedrine	**M2**	M2	Oxidation	$C_{11}H_{17}NO_2$	196.133 1	−0.4	9.79	66.2
P21	(−)-*N*-Methylephedrine	**M3**	M3	Oxidation	$C_{11}H_{17}NO_2$	196.133 1	−0.3	10.45	72.4
P21	(−)-*N*-Methylephedrine	**P12**	Norephedrine	Loss of CH_2 and CH_2	$C_9H_{13}NO$	152.106 9	−0.8	7.30	78.9
P21	(−)-*N*-Methylephedrine	**P13**	Norpseudoephedrine	Loss of CH_2 and CH_2	$C_9H_{13}NO$	152.106 8	−0.9	7.81	87.1
P21	(−)-*N*-Methylephedrine	**P16**	Ephedrine	Loss of CH_2	$C_{10}H_{15}NO$	166.122 5	−0.8	8.86	92.4
P21	(−)-*N*-Methylephedrine	**P18**	Pseudoephedrine	Loss of CH_2	$C_{10}H_{15}NO$	166.122 5	−1.1	9.04	91.0
P45	Dihydrocinnacasside	**P83**	3-(2-Hydroxyphenyl)propanoic acid	Loss of $C_6H_{10}O_5$	$C_9H_{10}O_3$	165.056 0	1.6	14.31	65.2
P16	Ephedrine	**M4**	M4	Glucuronidation	$C_{16}H_{23}NO_7$	342.155 2	1.4	2.81	51.1
P18	Pseudoephedrine	**M4**	M4	Glucuronidation	$C_{16}H_{23}NO_7$	342.155 2	1.4	2.81	51.1
P16	Ephedrine	**P12**	Norephedrine	Loss of CH_2	$C_9H_{13}NO$	152.106 9	−0.8	7.30	80.3
P18	Pseudoephedrine	**P12**	Norephedrine	Loss of CH_2	$C_9H_{13}NO$	152.106 9	−0.8	7.30	80.3
P16	Ephedrine	**P13**	Norpseudoephedrine	Loss of CH_2	$C_9H_{13}NO$	152.106 8	−0.9	7.81	87.1
P18	Pseudoephedrine	**P13**	Norpseudoephedrine	Loss of CH_2	$C_9H_{13}NO$	152.106 8	−0.9	7.81	87.1
P16	Ephedrine	**P21**	(−)-*N*-Methylephedrine	Methylation	$C_{11}H_{17}NO$	180.138 2	−0.6	9.45	69.9
P18	Pseudoephedrine	**P21**	(−)-*N*-Methylephedrine	Methylation	$C_{11}H_{17}NO$	180.138 2	−0.6	9.45	69.9
P16	Ephedrine	**P8**	OH-Ephedrine	Oxidation	$C_{10}H_{15}NO_2$	182.117 6	0.5	5.65	61.1
P18	Pseudoephedrine	**P8**	OH-Ephedrine	Oxidation	$C_{10}H_{15}NO_2$	182.117 6	0.5	5.65	61.1
P16	Ephedrine	**P9**	OH-Ephedrine	Oxidation	$C_{10}H_{15}NO_2$	182.117 6	0.5	6.09	61.1
P18	Pseudoephedrine	**P9**	OH-Ephedrine	Oxidation	$C_{10}H_{15}NO_2$	182.117 6	0.5	6.09	61.1
P41	*N*-Benzoylaspartic acid	**M5**	M5	Loss of O + Methylation	$C_{12}H_{13}NO_4$	236.091 7	0.1	14.99	51.1
P12	Norephedrine	**M6**	M6	*N*-Acetylation	$C_{11}H_{15}NO_2$	194.117 6	0.4	12.32	83.6
P13	Norpseudoephedrine	**M6**	M6	*N*-Acetylation	$C_{11}H_{15}NO_2$	194.117 6	0.4	12.32	83.6
P12	Norephedrine	**M7**	M7	*N*-Acetylation	$C_{11}H_{15}NO_2$	194.117 5	−0.2	12.52	50.0
P13	Norpseudoephedrine	**M7**	M7	*N*-Acetylation	$C_{11}H_{15}NO_2$	194.117 5	−0.2	12.52	50.0
P12	Norephedrine	**M8**	M8	*N*-Acetylation	$C_{11}H_{15}NO_2$	194.117 4	−0.6	14.08	64.0
P13	Norpseudoephedrine	**M8**	M8	*N*-Acetylation	$C_{11}H_{15}NO_2$	194.117 4	−0.6	14.08	64.0
P12	Norephedrine	**P16**	Ephedrine	Methylation	$C_{10}H_{15}NO$	166.122 5	−0.8	8.86	78.7
P13	Norpseudoephedrine	**P16**	Ephedrine	Methylation	$C_{10}H_{15}NO$	166.122 5	−0.8	8.86	78.7
P12	Norephedrine	**P18**	Pseudoephedrine	Methylation	$C_{10}H_{15}NO$	166.122 5	−1.1	9.04	77.4
P13	Norpseudoephedrine	**P18**	Pseudoephedrine	Methylation	$C_{10}H_{15}NO$	166.122 5	−1.1	9.04	77.4
P55	*O*-Coumaric acid glucoside	**P89**	4-Hydroxycinnamic acid	Loss of $C_6H_{10}O_5$	$C_9H_8O_3$	163.040 2	0.9	14.76	58.3
P32	*p*-Coumaric acid glucoside	**P89**	4-Hydroxycinnamic acid	Loss of $C_6H_{10}O_5$	$C_9H_8O_3$	163.040 2	0.9	14.76	58.3

while others could experience the biotransformation. There were eight newly bio-transform metabolites being observed in the plasma and brain, mainly from ephedra alkaloids, and the biotransformation pathway of (−)-*N*-methylephedrine was presented in Fig. 4. Based on ephedrine and its isomers' cleavage pathway and the losing mass ion deviation, the biotransformation of ephedrine and its isomers mainly concluded methylation, glucuronidation, oxidation and *N*-acetylation.

3.5.2. Drug-time curve of MGD

In the previous sections, we had proved that some prototypes and their metabolites could be absorbed into plasma and brain. We further explored the concentration of those constitutions *in vivo*. As for prototypes, their plasma concentration could accumulate immediately and reach their peak between 15–60 min, and then following with excretion. Four of them, namely 3-(2-hdroxyphenyl) propanoic acid, ephedrine derivative, 4-hydroxycinnamic acid and *trans*-cinnamic acid presented an upward trend again. We speculated this situation was caused by the metabolism from the other prototype or the hepatoenteral circulation. As for the prototypes in brain, their concentration also showed a similar tendency. Half of them kept at a plateau before excretion (Figs. 5 and 6).

To sum up, most of prototypes of MGD absorbed in blood could get to their blood concentration peek rapidly, and then go through elimination. Some of them could keep at a relatively high concentration for a short time, and part of them could be secondary absorption. While the prototypes distributed in brain got to their concentration peek around 15 to 30 min later than those in blood. Additionally, most of them could remain a stable concentration for a longer period before elimination in brain, that is, they might take a longer pharmacological action in brain.

As for metabolites, the identified metabolites in plasma presented an upward tendency in the first 15 min and kept at a high plasma concentration, while M1 increased to its maximum at 90 min. After that, the metabolites excreted gradually. Owing to

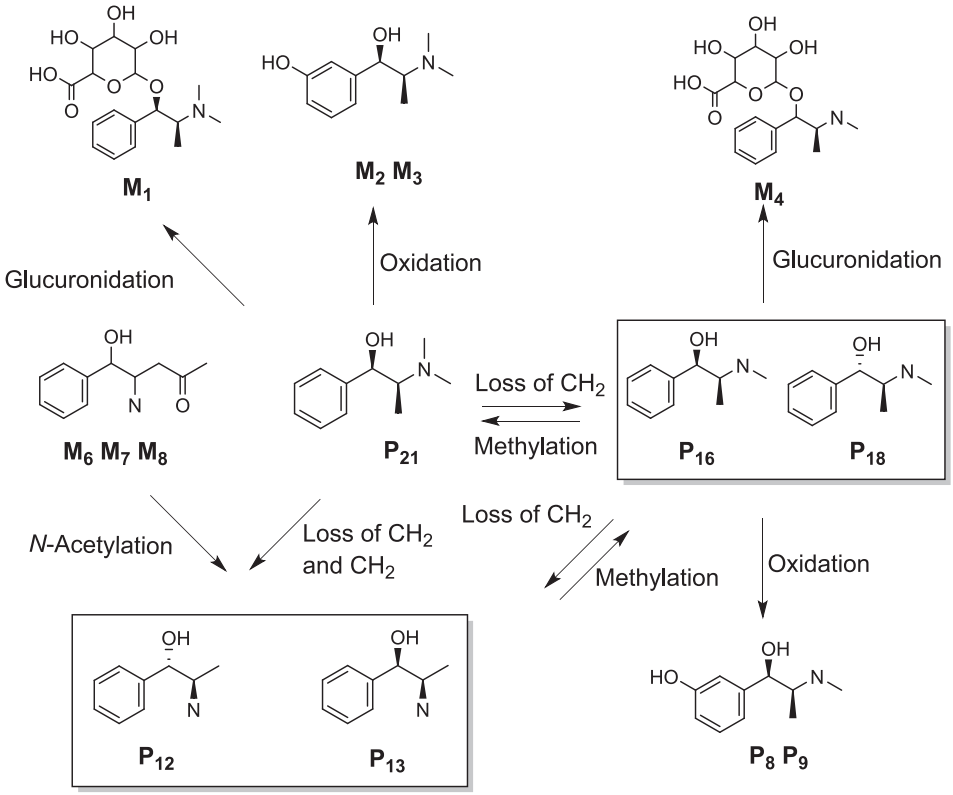

Fig. 4. Bio-transform pathway of (−)-*N*-methylephedrine *in vivo*.

a short collecting period, we could only observe the absorption of ten prototypes and four metabolites in brain (Figs. 7 and 8).

Overall, the metabolites detected either in plasma or in brain could remain longer time than prototype ones, except for the M1 in blood, which means the metabolites could also be the bioactive constituents of MGD.

3.6. Quanlity control of MGD

According to *Chinese pharmacopoeia* (version 2020), it regulates that the content determinations of EH by analyzing ephedrine and pseudoephedrine, while cinnamaldehyde for CR. However, those compounds are chosen owing to high content or being representative, without considering their pharmacological effects. Moreover, cinnamaldehyde is categorized as a volatile compound, which is easy volatilized during water extraction under high temperature (Otoni et al., 2014). In TCM therapy, water boiling is the easiest and widest using method to prepare TCM prescription. In our research, we focused the compounds in MGD *in vivo* based on its water extraction corresponded to our previous study (Wei et al., 2017), cinnamaldehyde was not detected in our study, while *trans*-cinnamic acid was identified both in MGD and blood sample. Moreover, it had been reported that cinnamaldehyde could transform to *trans*-cinnamic acid by oxidation in the body (Sun et al., 2018). Therefore, based on our research, we speculated that ephedrine, pseudoephedrine and *trans*-cinnamic acid could be the quanlity indicator of MGD. These three coumpouds would be further studied in next step.

4. Conclusion

In our study, UPLC-Q-TOF-MS technique successfully helped us to characterize the chemical constituents in MGD and the absorption and distribution of the prototypes and metabolites of MGD in plasma and brain, including eight metabolites in plasma and four in brain. We also discovered that those constituents of MGD detected *in vivo* could be absorbed in plasma and distributed in brain rapidly, which provided the scientific evidence for further exploration the bioactive constituents of MGD.

CRediT authorship contribution statement

Ping Wei: Conceptualization, Methodology, Resources, Writing – original draft, Funding acquisition. **Shiying Huang:** Writing – original draft, Visualization, Investigation. **Juan Yang:** Methodology, Formal analysis. **Mo Zhao:** Formal analysis. **Qiugu Chen:** Investigation. **Xiaoyu Deng:** Data curation. **Jianping Chen:** Methodology, Supervision, Funding acquisition. **Yisheng Li:** Methodology, Funding acquisition, Writing – review & editing.

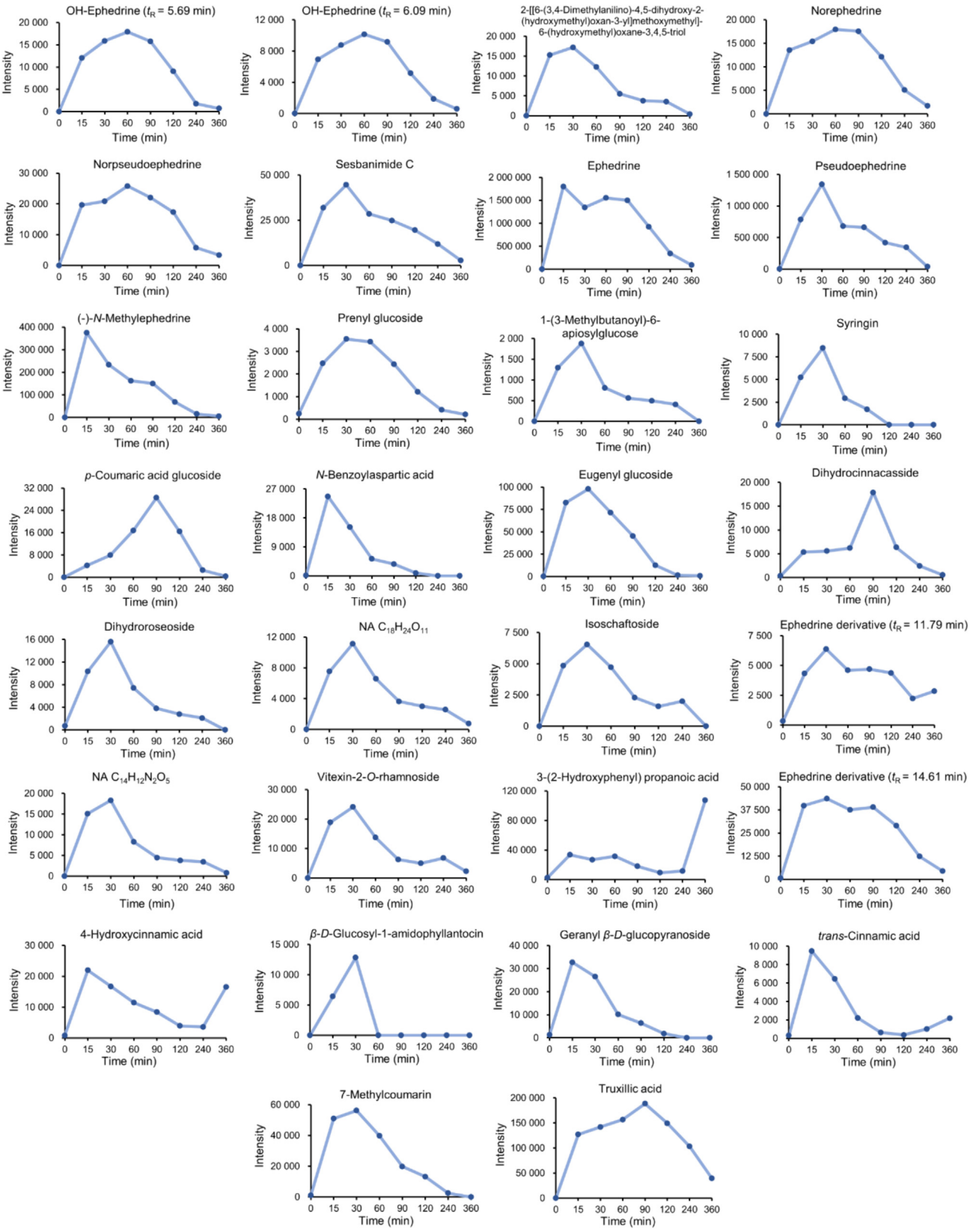

Fig. 5. Drug-time curves of prototype constituents detected in plasma.

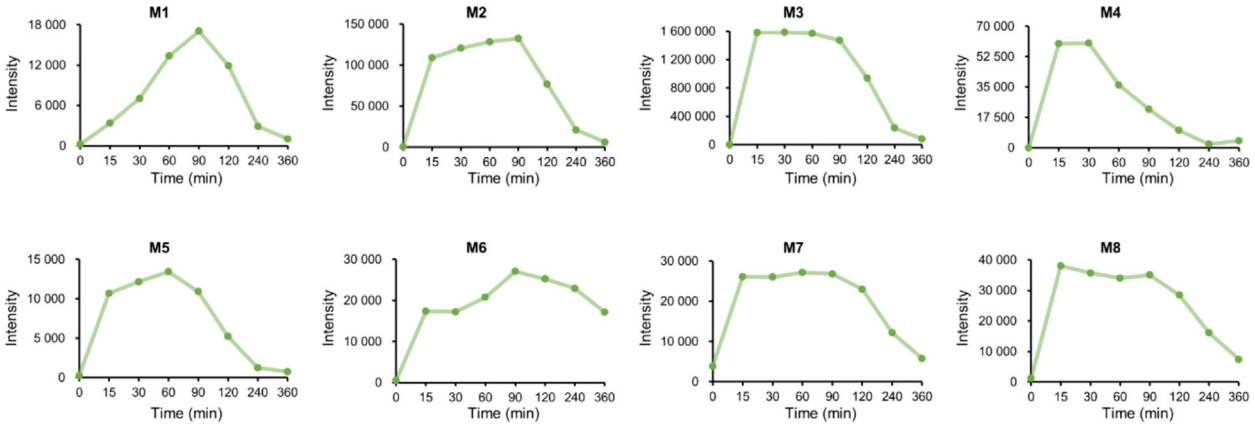

Fig. 6. Drug-time curves of metabolites detected in brain.

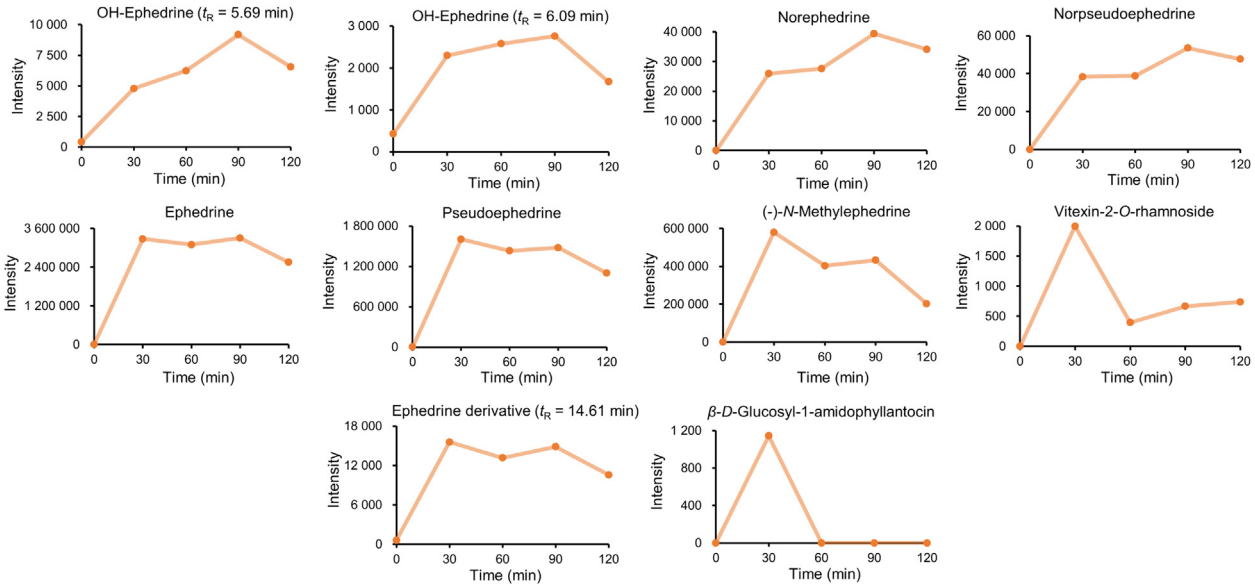

Fig. 7. Drug-time curves of prototype constituents detected in brain.

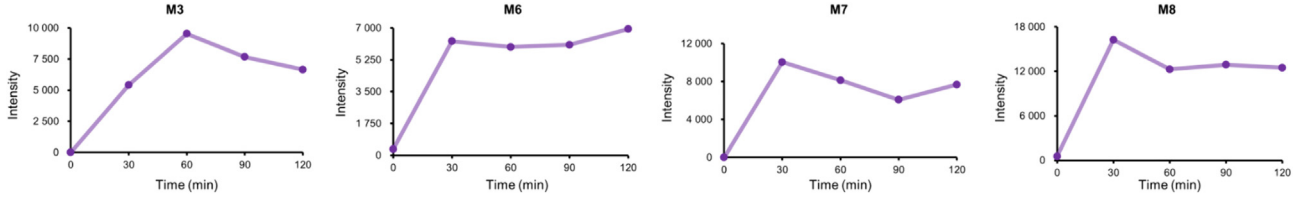

Fig. 8. Drug-time curve of metabolites detected in brain.

Declaration of Competing Interest

The authors declare that they have no known competing financial interests or personal relationships that could have appeared to influence the work reported in this paper.

Acknowledgements

This work was supported by Shenzhen Science and Technology Program (No. JCYJ20210324140204011), Shenzhen Science and Technology Program (No. JSGG20210802093208023), Shenzhen Science and Technology Program (No. ZDSYS201606081515458), Foundation of Guangdong Provincial Key Laboratory of Functional Substances in Medicinal Edible Resources and Healthcare Products (No. GPKLFSHP202101), and the Sanming Project of Medicine in Shenzhen (No. SZZYSM202111002).

Appendix A. Supplementary material

Supplementary material to this article can be found online at https://doi.org/10.1016/j.chmed.2024.01.006.

References

Abrankó, L., García-Reyes, J. F., & Molina-Díaz, A. (2011). In-source fragmentation and accurate mass analysis of multiclass flavonoid conjugates by electrospray ionization time-of-flight mass spectrometry. *Journal of Mass Spectrometry, 46*(5), 478–488.

Chen, L., Yao, C. L., Li, J., Wang, J. Y., Yao, S., Shen, S. J., Yang, L., Zhang, J. Q., Wei, W. L., Bi, Q. R., & Guo, D. A. (2021). Systematic characterization of chemical constituents in Mahuang decoction by UHPLC tandem linear ion trap-Orbitrap mass spectrometry coupled with feature-based molecular networking. *Journal of Separation Science, 44*(14), 2717–2727.

Fan, H. S., Liu, S. J., Shen, W. X., Kang, A., Tan, J. N., Li, L., Liu, X., Xu, C. L., Xu, X. F., Lai, Y. Y., Cheng, H. B., & Sun, D. D. (2020). Identification of the absorbed components and metabolites of Xiao-Ai-Jie-Du decoction and their distribution in rats using ultra high-performance liquid chromatography/quadrupole time-of-flight mass spectrometry. *Journal of Pharmaceutical and Biomedical Analysis, 179*, 112984.

Fu, Y. J., Yan, Y. Q., Qin, H. Q., Wu, S., Shi, S. S., Zheng, X., Wang, P. C., Chen, X. Y., Tang, X. L., & Jiang, Z. Y. (2018). Effects of different principles of traditional Chinese medicine treatment on TLR7/NF-κB signaling pathway in influenza virus infected mice. *Chinese Medicine, 13*(1), 42.

Kim, B. Y., Cao, L. H., & Kim, J. Y. (2011). Common responses in gene expression by *Ephedra herba* in brain and heart of mouse. *Phytotherapy Research, 25*(10), 1440–1446.

Krizevski, R., Bar, E., Shalit, O., Sitrit, Y., Ben-Shabat, S., & Lewinsohn, E. (2010). Composition and stereochemistry of ephedrine alkaloids accumulation in *Ephedra sinica* Stapf. *Phytochemistry, 71*(8–9), 895–903.

Lin, B. F., Guo, S. J., Hong, X. X., Jiang, X. Y., Li, H. W., Li, J. W., Guo, L. L., Li, M. L., Chen, J. P., Huang, B., & Xu, Y. F. (2022). Chemical characterization and metabolic profiling of the compounds in the Chinese herbal formula Li Chang decoction by UPLC-QTOF/MS. *Evidence-Based Complementary and Alternative Medicine, 2022*, 1322751.

Liu, J., Zhang, Q., Li, R. L., Wei, S. J., Huang, C. Y., Gao, Y. X., & Pu, X. F. (2020). The traditional uses, phytochemistry, pharmacology and toxicology of *Cinnamomi ramulus*: A review. *Journal of Pharmacy and Pharmacology, 72*(3), 319–342.

Liu, W., Huang, J., Zhang, F., Zhang, C. C., Li, R. S., Wang, Y. L., Wang, C. R., Liang, X. M., Zhang, W. D., Yang, L., Liu, P., & Ge, G. B. (2021). Comprehensive profiling and characterization of the absorbed components and metabolites in mice serum and tissues following oral administration of Qing-Fei-Pai-Du decoction by UHPLC-Q-Exactive-Orbitrap HRMS. *Chinese Journal of Natural Medicines, 19*(4), 305–320.

Mu, X. M., Xu, X. K., Guo, X., Yang, P. M., Du, J., Mi, N., Cheng, T. F., Lu, L., Qi, X. P., Wang, X. Y., Ning, J., Zhang, W. D., & Ye, J. (2019). Identification and characterization of chemical constituents in Dengzhan Shengmai Capsule and their metabolites in rat plasma by ultra-performance liquid chromatography coupled with quadrupole time-of-flight mass spectrometry. *Journal of Chromatography B, 1108*, 54–64.

Niu, B., Zheng, F. H., & Xu, J. P. (2020). Protective effect of gui zhi (Ramulus Cinnamomi) on abnormal levels of four amino acid neurotransmitters by chronically ma huang (*Herb Ephedra*) intoxicated prefrontal cortex in rats treated with a ma huang-gui zhi herb pair. *Journal of Ethnopharmacology, 249*, 112408.

Otoni, C. G., Moura, M. R., Aouada, F. A., Camilloto, G. P., Cruz, R. S., Lorevice, M. V., Soares, N. F., & Mattoso, L. H. C. (2014). Antimicrobial and physical-mechanical properties of pectin/papaya puree/cinnamaldehyde nanoemulsion edible composite films. *Food Hydrocolloids, 41*, 188–194.

Serafini, M., Peluso, I., & Raguzzini, A. (2010). Flavonoids as anti-inflammatory agents. *Proceedings of the Nutrition Society, 69*(3), 273–278.

Sun, Q., Yang, H., Tang, P., Liu, J., Wang, W., & Li, H. (2018). Interactions of cinnamaldehyde and its metabolite cinnamic acid with human serum albumin and interference of other food additives. *Food Chemistry, 243*, 74–81.

Tang, S. Y., Ren, J. L., Kong, L., Yan, G. L., Liu, C., Han, Y., Sun, H., & Wang, X. J. (2023). *Ephedrae herba*: A review of its phytochemistry, pharmacology, clinical application, and alkaloid toxicity. *Molecules, 28*(2), 663.

Vogt, T. (2010). Phenylpropanoid biosynthesis. *Molecular Plant, 3*(1), 2–20.

Wan, H. Y., Pan, L. J., Wang, Y., Li, C., Yu, L., Zhou, H. F., Wan, H. T., & He, Y. (2020). Pharmacokinetics of seven major active components of Mahuang decoction in rat blood and brain by LC-MS/MS coupled to microdialysis sampling. *Naunyn-Schmiedeberg's Archives of Pharmacology, 393*(8), 1559–1571.

Wei, P., Huo, H. L., Ma, Q. H., Li, H. C., Xing, X. F., Tan, X. M., & Luo, J. B. (2014). Pharmacokinetic comparisons of five ephedrine alkaloids following oral administration of four different Mahuang-Guizhi herb-pair aqueous extracts ratios in rats. *Journal of Ethnopharmacology, 155*(1), 642–648.

Wei, P., Tang, Q. F., Huo, H. L., Chen, F. L., Song, S., Xing, X. F., & Luo, J. B. (2017). Comparative pharmacokinetics of three phenylpropanoids in rat plasma after oral administration of *Ramulus Cinnamomi* and *Ramulus Cinnamomi-Ephedrae Herba* herb-couple extract. *Chinese Journal of Integrative Medicine, 2017*, 1–7.

Xiang, H. J., Zhang, L. S., Song, J. N., Fan, B., Nie, Y. L., Bai, D., & Lei, H. M. (2016). The profiling and identification of the absorbed constituents and metabolites of Guizhi decoction in rat plasma and urine by rapid resolution liquid chromatography combined with quadrupole-time-of-flight mass spectrometry. *International Journal of Molecular Sciences, 17*(9), 1409.

Xu, L., Liu, Y., Wu, H. F., & Zhou, A. (2020). Rapid identification of absorbed components and metabolites of Gandou decoction in rat plasma and liver by UPLC-Q-TOF-MS^{E}. *Journal of Chromatography B, 1137*, 121934.

Yuan, H. J., Li, W., Jin, J. M., Chen, J. J., Jiang, J., Wang, H., Jia, X. B., & Feng, L. (2017). Research progress on chemical constituents, pharmacological mechanism and clinical application of Guizhi decoction. *China Journal of Chinese Materia Medica, 42*(23), 4556–4564.

Zang, X. Y., Shang, M. Y., Xu, F., Liang, J., Wang, X., Mikage, M., & Cai, S. Q. (2013). A-type proanthocyanidins from the stems of *Ephedra sinica* (Ephedraceae) and their antimicrobial activities. *Molecules, 18*(5), 5172–5189.

Zhang, C. L., Fan, L. H., Fan, S. M., Wang, J. Q., Luo, T., Tang, Y., Chen, Z. M., & Yu, L. Y. (2019). *Cinnamomum cassia* Presl: A review of its traditional uses, phytochemistry, pharmacology and toxicology. *Molecules, 24*(19), 3473.

Zheng, F. H., Wei, P., Huo, H. L., Xing, X. F., Chen, F. L., Tan, X. M., & Luo, J. B. (2015). Neuroprotective effect of Gui Zhi (*Ramulus Cinnamomi*) on Ma Huang- (*Herb Ephedra*-) induced toxicity in rats treated with a Ma Huang-Gui Zhi herb pair. *Evidence-Based Complementary and Alternative Medicine, 2015*, 913461.

Zheng, Q. G., Mu, X. Y., Pan, S. B., Luan, R. Q., & Zhao, P. (2023a). *Ephedrae herba*: A comprehensive review of its traditional uses, phytochemistry, pharmacology, and toxicology. *Journal of Ethnopharmacology, 307*, 116153.

Zheng, Y. X., Wang, Y. Y., Wang, L., Wang, Y. M., Wei, J. X., & Li, Y. B. (2023b). Modern research and thinking on compatibility mechanism of reducing toxicity of traditional Chinese medicine. *Chinese Traditional and Herbal Drugs, 54*(2), 386–395.